Ferroelectric rods with adjustable dielectric tunability

Yue Zheng[a] and C. H. Woo[b]
Department of Electronic and Information Engineering, The Hong Kong Polytechnic University, Hong Kong SAR, China

Biao Wang[c] and Z. Y. Zhu
Electro-Optics Technology Center, Harbin Institute of Technology, Harbin, China

(Received 22 November 2006; accepted 24 January 2007; published online 2 March 2007)

The polarization, dielectric constant, and tunability of a radial-loaded ferroelectric rod inside a highly pressurized polyethylene tube are calculated for both macro- and nanodimensions within a thermodynamic model. All studied properties, including the Curie temperature, are found to vary substantially by the applied load. The authors' results indicate that many properties of the ferroelectric rod, including its tunability, can be optimized in this design by adjusting the applied pressure. © *2007 American Institute of Physics*. [DOI: 10.1063/1.2709899]

Ferroelectric materials are useful in many applications such as electrooptic devices, ultrahigh density memory devices, tunable microwave devices, and other microelectronic, nonvolatile memories, etc. The development of tunable dielectric materials for voltage controlled, frequency-agile phase shifters and filters operating in the microwave devices is of particular interest.[1–11]

A ferroelectric rod with radius R and height h is placed inside a high-pressure polyethylene (HPPE) tube as shown in Fig. 1. SH in Fig. 1 is a stiff cylindrical steel housing,[12] and the entire arrangement is called a S-H-F system. An applied axial compressive stress σ_z on the HPPE translates into a uniform compressive radial stress σ_r on the rod, which combines with the surface tension σ_r^s to give the total radial stress σ_r^t as[10–13]

$$\sigma_r^t = \sigma_r^s + \sigma_r, \tag{1}$$

with $\sigma_r^s = -\mu/R$ and $\sigma_r = (v/1-v)\sigma_z = -(v/1-v)p$, where μ is the surface tension coefficient and v the Poisson ratio of HPPE. p is the value of the applied axial pressure.

We use a cylindrical coordinate system in which the major component of the polarization is along the z direction. Taking into account the combined effects of the applied stress, the depolarization field, and applied electric field, the total free energy of ferroelectric rod in cylindrical coordinates (r, φ, z) is given by[9–11]

$$F = 2\pi \int_0^h dz \int_0^R rdr \left\{ \frac{\alpha_\sigma(T)}{2} P^2(r,z) + \frac{\beta}{4} P^4(r,z) + \frac{\gamma}{6} P^6(r,z) + \frac{D}{2} [\nabla P(r,z)]^2 - \frac{1}{2} E_d P(r,z) - E_{\text{ext}} P(r,z) - (s_{11}+s_{12}) \left(\frac{\mu}{R} + \frac{v}{1-v} p \right)^2 \right\} + F_s, \tag{2}$$

where β, γ, and D are the free-energy expansion coefficients of the corresponding bulk material. $E_d(z)$ is the depolarization field and $E_{\text{ext}}(z)$ is the external field.[10]

The free-energy expansion coefficient $\alpha_\sigma(T)$ in Eq. (2) can be written as

$$\alpha_\sigma(T,R,p) = \alpha(T - T_{c0}) + 4Q_{12} \left(\frac{\mu}{R} + \frac{v}{1-v} p \right), \tag{3}$$

where α is proportional to the inverse Curie constant known for the bulk material. T_{c0} is the Curie temperature of the bulk crystal. Q_{12} are the components of the electrostrictive tensor. s_{11} and s_{12} are components of the elastic compliance tensor. F_s is the energy associated with the lattice relaxation on the surface that includes the planar end surfaces and the curved sidewall. We assume that F_s can be empirically represented via the corresponding extrapolation lengths $\delta_{\text{u-p}}$ and $\delta_{\text{s-w}}$ and expressed in the following form:

$$F_s = D \int_0^R \frac{2\pi r}{\delta_{u\text{-}p}} dr [P^2(r, z = h/2) + P^2(r, z = -h/2)] + D \int_{-h/2}^{-h/2} \frac{2\pi R}{\delta_{s\text{-}w}} dz P^2(r = R, z). \tag{4}$$

Using direct variational method, the polarization field $P(r)$ under an applied electric field E_{ext} can be obtained by solving the following Euler-Lagrange equation:[10–13]

$$\delta F / \delta P = 0. \tag{5}$$

The surface term in Eq. (4) yields the boundary conditions $\partial P / \partial z = \mp P / \delta_{u\text{-}b}|_{z=\pm h/2}$ and $\partial P / \partial r = - P / \delta_{s\text{-}w}|_{r=R}$.

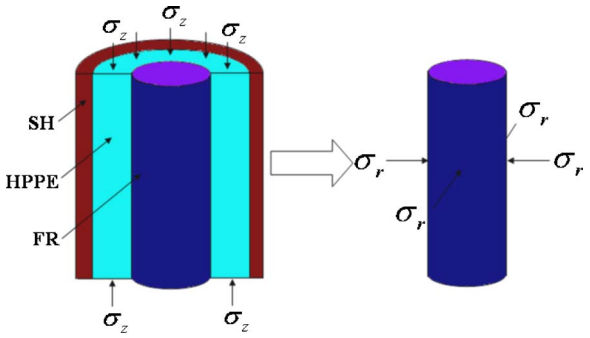

FIG. 1. (Color online) Schematic of the ferroelectric rod in S-H-F system.

[a]Also at Electro-Optics Technology Center, Harbin Institute of Technology, Harbin, China; electronic mail: yuezheng@hit.edu.cn
[b]Author to whom correspondence should be addressed; electronic mail: chung.woo@polyu.edu.hk
[c]Also at State Key Laboratory of Optoelectronic Materials and Technologies, Sun Yat-sen University, Guangzhou, China; electronic mail: stdwangb@zsu.edu.cn

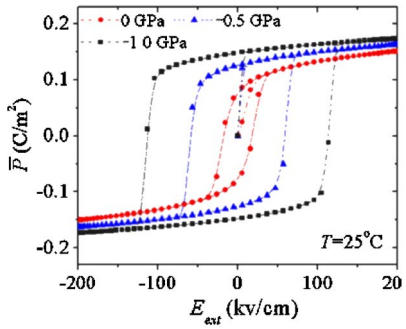

FIG. 2. (Color online) Hysteresis loops in ferroelectric rod with different applied axial compressive stresses at $T=25\ ^{\circ}\mathrm{C}$ ($T<T_{c0}$).

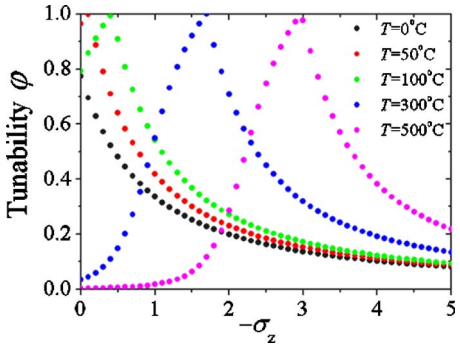

FIG. 4. (Color online) Relation between the applied axial compressive stresses (GPa) and tunability of BST(70/30) ferroelectric rod under an applied field $E_{\mathrm{ext}}=100$ kV/cm.

In the following, we use as an example the $Ba_mSr_{1-m}TiO_3$ (BST) material system commonly used in dielectric devices, with material constants from the literatures.[10–15] We first consider a macroscopic BST ferroelectric rod with a radius so large that surface effects in the free energy in Eq. (2) can be neglected.[15] At the same time, we assume that the length h of the rod is much larger than its radius R, such as $h/2R=10$. We use the depolarization field due to the end electrodes derived in Refs. 10 and 11.

Hysteresis loops for different applied pressures at room temperature caused by a sinusoidal external electric field $E_{\mathrm{ext}}=E_0\sin(2\pi\omega t)$ are shown in Fig. 2. Here E_0 and ω are the amplitude and circular frequency, respectively. It can be seen that both the remnant polarization P_r and the coercive field E_c clearly increase with the applied pressure for temperature T being below the Curie temperature. Moreover, for temperature T being above the Curie temperature, the relation between the polarization P and the external field E_{ext} is only linear at $\sigma_z=0$. With the increasing applied pressure, the hysteresis loops appear, such as $\sigma_z=-1.5$, -2.0, and -2.5 GPa, and the remnant polarization P_r and the coercive field E_c clearly increase with the applied pressure.

Solving the polarization field from Eq. (5), the dielectric constant $\varepsilon(E_{\mathrm{ext}})$ can be obtained by evaluating $(\partial^2 f/\partial P^2)^{-1}$, where f is the local energy density. Figures 3(a) and 3(c) show the calculated polarization and dielectric constants for various temperatures in the absence of the external field. Below the Curie temperature, the BST rod at $T=0\ ^{\circ}\mathrm{C}$ is ferroelectric for the full range of applied pressure. For temperatures above the Curie temperature of 34 °C, switchable para-/ferroelectric phases accompanied by strong variations of the dielectric constant in the rod are seen to be achievable by varying the applied pressure. Even under an external electric field of $E_{\mathrm{ext}}=100$ kV/cm, the polarization and dielectric constant of ferroelectric rod are still very much changed by the applied pressure at all operating temperatures under consideration [Figs. 3(b) and 3(d)].

In this work, the tunability is defined as the ratio of the variation of the dielectric constant at a given applied electric field E_{ext} to the dielectric constant at zero bias,[4,7,8] $\varphi(E_{\mathrm{ext}})=[\varepsilon(E_{\mathrm{ext}}=0)-\varepsilon(E_{\mathrm{ext}})]/\varepsilon(E_{\mathrm{ext}}=0)$. The BST rod in S-H-F system is assumed to be under an applied electric field $E_{\mathrm{ext}}=100$ kV/cm along the z direction. Repeating the foregoing calculations, we plot the results in Fig. 4 to show the tunability of the BST rod as functions of the applied pressure at various temperatures $T=0$, 50, 100, 300, and 500 °C. It is evident that the tunability is controllable by varying the applied pressure. Moreover, it is very interesting that for the

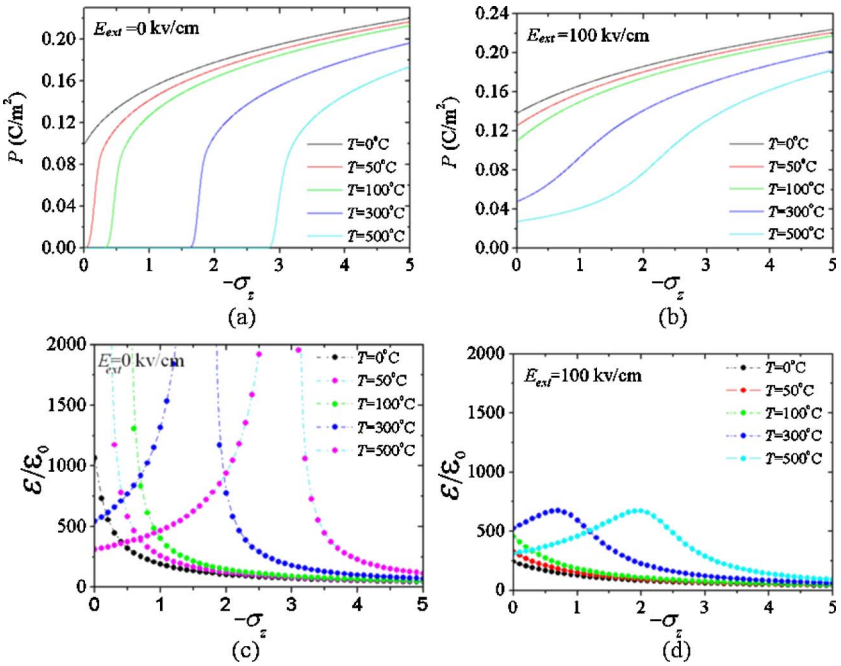

FIG. 3. (Color online) Relation between the applied axial compressive stresses (GPa) and the polarization at E_{ext} of (a) 0 kV/cm and (b) 100 kV/cm. The relation between the applied axial stresses and the relative dielectric constant at E_{ext} of (c) 0 kV/cm and (d) 100 kV/cm.

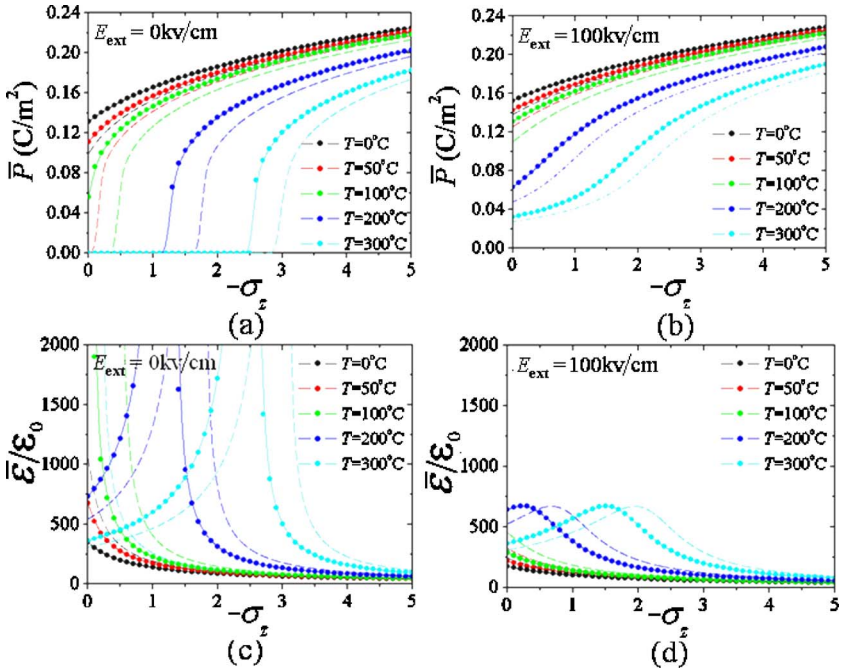

FIG. 5. (Color online) For nanorod (R=50 nm), the relation between the applied axial compressive stresses (GPa) and the polarization at E_{ext} of (a) 0 kV/cm and (b) 100 kV/cm. The relation between the applied axial stresses and the relative dielectric constant at E_{ext} of (c) 0 kV/cm and (b) 100 kV/cm. (Dash lines are results in Fig. 3.)

S-H-F system, the tunability can be optimized through the applied axial stress σ_z.

In the nanoscale, the surface effects are important in the free energy in Eq. (2). We consider a ferroelectric nanorod with a radius of R=50 nm and a length h=20R. Minimization of the total free energy F in Eq. (2) with respect to P gives the stationary values of P and boundary conditions. In our calculation, the values of the effective surface tension coefficient and extrapolation length are 20 N/m and 30 nm, respectively,[10,11,14] corresponding to a surface tension of 0.4 GPa in the present case.

Figures 5(a) and 5(c) show the average polarization and dielectric constants for various temperatures in the absence of the external field. These results show that the surface tension enhances the polarization and increases the Curie temperature for the nanorod. Under external electric fields of 0 and 100 kV/cm, the polarization and dielectric constant of the ferroelectric rod are still very sensitive to the applied pressure at all operating temperatures investigated [Figs. 5(b) and 5(d)]. We also calculate the tunability as a function of the applied pressure at various temperatures T=0, 50, 100, 300, and 500 °C (Fig. 6). Comparing with Fig. 4 for a macroscopic rod, it can be seen that the sensitivity of the tunability as a function of applied axial stress σ_z for a nanorod is only slightly reduced, due to the interference of the large surface tension.

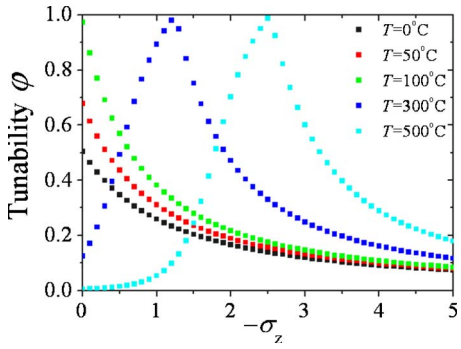

FIG. 6. (Color online) For nanorod (R=50 nm), the relation between the applied axial compressive stresses (GPa) and tunability.

In summary, the polarization, dielectric constant, and tunability of ferroelectric rods in a S-H-F system are calculated within a thermodynamic model. We found that when applied above the Curie temperature, para-/ferroelectric phases can be switchable by varying the applied pressure, accompanied by a large change of the dielectric constant. As a result, the tunability and other dielectric properties of the rod can be optimized by adjusting the applied pressure.

This project was supported by grants from the Research Grants Council of the Hong Kong Special Administrative Region (PolyU5312/03E and 5322/04E). One of the authors (B.W.) is also grateful for support from the National Science Foundation of China (Nos. 50232030, 10172030, and 10572155) and the Science Foundation of Guangzhou Province (2005A10602002).

[1] A. K. Tagantsev, V. O. Sherman, K. F. Astafiev, J. Venkatesh, and N. Setter, J. Electroceram. **11**, 5 (2003).
[2] Y. Zheng, B. Wang, and C. H. Woo, Appl. Phys. Lett. **89**, 062904 (2006).
[3] A. Amin, J. Electroceram. **8**, 99 (2002).
[4] A. Sharma, Z. G. Ban, S. P. Alpay, and J. V. Mantese, Appl. Phys. Lett. **85**, 985 (2004).
[5] B. Wang and C. H. Woo, J. Appl. Phys. **100**, 044114 (2006).
[6] W. K. Simon, E. K. Akdogan, A. Safari, and J. Bellotti, Appl. Phys. Lett. **88**, 132902 (2006).
[7] Z. G. Ban and S. P. Alpay, J. Appl. Phys. **91**, 504 (2003).
[8] Z. G. Ban and S. P. Alpay, J. Appl. Phys. **91**, 9288 (2002).
[9] B. Wang and C. H. Woo, J. Appl. Phys. **97**, 084109 (2005).
[10] A. N. Morozovska, E. A. Eliseev, and M. D. Glinchuk, Phys. Rev. B **73**, 214106 (2006).
[11] A. N. Morozovskaya, E. A. Eliseev, and M. D. Glinchuk, Physica B **322**, 356 (2006).
[12] T. Granzow, A. B. Kounga, E. Aulbach, and J. Rodel, Appl. Phys. Lett. **88**, 252907 (2006).
[13] H. T. Huang, C. Q. Sun, T. S. Zhang, and H. Peter, Phys. Rev. B **63**, 184112 (2001).
[14] Y. Zheng, B. Wang, and C. H. Woo, Appl. Phys. Lett. **89**, 083115 (2006).
[15] Z. G. Ban, S. P. Alpay, and J. V. Mantese, Phys. Rev. B **67**, 184104 (2003).